

**Drone-Assisted Cellular Networks  
Optimal Positioning and Load Management**

Pijnappel, T. R.; Van Den Berg, J. L.; Borst, S. C.; Litjens, R.

**DOI**

[10.1109/VTC2021-Spring51267.2021.9448643](https://doi.org/10.1109/VTC2021-Spring51267.2021.9448643)

**Publication date**

2021

**Document Version**

Accepted author manuscript

**Published in**

2021 IEEE 93rd Vehicular Technology Conference, VTC 2021-Spring - Proceedings

**Citation (APA)**

Pijnappel, T. R., Van Den Berg, J. L., Borst, S. C., & Litjens, R. (2021). Drone-Assisted Cellular Networks: Optimal Positioning and Load Management. In *2021 IEEE 93rd Vehicular Technology Conference, VTC 2021-Spring - Proceedings* Article 9448643 (IEEE Vehicular Technology Conference; Vol. 2021-April). IEEE. <https://doi.org/10.1109/VTC2021-Spring51267.2021.9448643>

**Important note**

To cite this publication, please use the final published version (if applicable).  
Please check the document version above.

**Copyright**

Other than for strictly personal use, it is not permitted to download, forward or distribute the text or part of it, without the consent of the author(s) and/or copyright holder(s), unless the work is under an open content license such as Creative Commons.

**Takedown policy**

Please contact us and provide details if you believe this document breaches copyrights.  
We will remove access to the work immediately and investigate your claim.

# Drone-Assisted Cellular Networks: Optimal Positioning and Load Management

T.R. Pijnappel\*, J.L. van den Berg<sup>†‡§</sup>, S.C. Borst\*, R. Litjens<sup>†¶</sup>

\*Eindhoven University of Technology, Eindhoven, The Netherlands

<sup>†</sup>TNO, The Hague, The Netherlands

<sup>‡</sup>University of Twente, Enschede, The Netherlands

<sup>§</sup>CWI, Amsterdam, The Netherlands

<sup>¶</sup>Delft University of Technology, Delft, The Netherlands

**Abstract**—The use of drone base stations offers an agile mechanism to safeguard coverage and provide capacity relief when cellular networks are under stress. Such stress conditions can occur for example in case of special events with massive crowds or network outages. In this paper we focus on a disaster scenario with emergence of a hotspot, and analyze the impact of the drone position (altitude, horizontal position) and selection bias on the network performance. We determine the optimal settings of these control parameters as a function of the hotspot location, and demonstrate that the optimized values can drastically reduce the fraction of failed calls.

**Index Terms**—Drone-assisted cellular networks, drone positioning, load management, performance assessment

## I. INTRODUCTION

Wireless cellular networks have become a critical infrastructure in today's digital society, and assurance of high reliability and quality is a key requirement for service providers. While networks are carefully engineered to provide reliable coverage and adequate capacity in nominal operating conditions, this can be compromised in certain atypical situations, e.g. festivals or sports games with huge crowds or network anomalies due to failures or disasters. The deployment of drone base stations provides an appealing approach to protect coverage and/or rapidly resolve capacity issues in such circumstances [1].

In order for the deployment of drone base stations to be effective in quite diverse and often unpredictable scenarios, several challenges need to be addressed however. In particular, the position of the drone will have a critical impact on the performance benefits. When properly positioned, the drone could significantly improve capacity/coverage, while a badly positioned drone could result in high interference and therefore degrading performance. A related challenge is to determine a good policy or selection bias for assigning users to a drone or regular base station in order to properly balance the loads. These challenges are exacerbated by the fact that it is not even clear what the key factors are that determine the optimal control parameter settings and to what extent these factors can be observed or estimated in practical deployments [1].

### A. Contributions

In this paper we focus on a network disruption event with a failing base station and emergence of a hotspot. As a way to restore service, we consider the deployment of a drone base

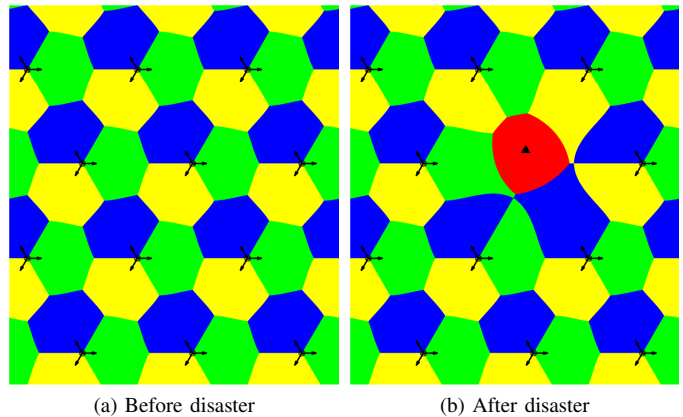


Fig. 1: Coverage regions before and after a disaster event and a consequent drone deployment. Green, blue and yellow areas indicate the cells of the regular base stations (black dots, where the arrows identify the azimuth directions) and the red cell is covered by the drone (black triangle).

station to handle some of the users that would have been served by the failing base station as illustrated in Figure 1. The Call Success Rate (CSR) (as defined in detail later) is adopted as a key performance metric to capture the efficacy of the drone in terms of coverage and capacity relief. Motivated by the above-mentioned challenges, we provide insights in 1) the impact of the drone position and selection bias on the CSR for various load scenarios, and 2) the optimal position and selection bias as well as the corresponding CSR as function of the location of the hotspot. These results offer a useful cornerstone for the design of adaptive and possibly data-driven algorithms for optimal parameter configuration and management of drone base stations.

### B. Related literature

The deployment of aerial base stations has attracted significant attention in recent years. In [2] the authors determine the optimal altitude of a drone for a given maximum allowed path loss. In [3] a comparison is made between a conventional terrestrial network and a drone-assisted network where the position of the drone is determined using Q-learning. The authors of [4] propose a Q-learning algorithm

for optimal drone positioning in an emergency scenario where the conventional network is completely destroyed. In a similar setting the authors of [5] use Q-learning to determine the best transmit power allocation and positioning of drones. In [6] the authors derive the optimal altitude and separation distance for the coverage of a rectangular area using two drones. In [7] three algorithms (Q-learning, a gradient-based technique and a greedy search) are considered for minimizing the maximum path loss. The authors in [8] propose a heuristic scheme to find the minimum number of drones and their optimal 3D positions in a scenario without any regular base station. In [9] an approach using multiple drones to form a communication ‘bridge’ is considered to offload excessive traffic demand to an underloaded base station.

As opposed to the above papers, our work considers a control parameter to steer traffic towards/away from a drone base station in order to properly balance the loads. To the best of our knowledge, this work is the first to consider such a selection bias, and provides explicit insight in the impact of the drone position and selection bias on the CSR. It is worth observing that this can come on top of cell outage compensation as a default method to maintain coverage [10].

### C. Organization of the paper

The remainder of the paper is organized as follows. In Section II we discuss a few key challenges related to the control parameters. In Section III we describe the specific network scenario that we consider. We then investigate in Section IV the impact of the selection bias and the drone position, followed by an analysis of the optimal settings of these parameters. In Section V we provide some concluding remarks and suggestions for further research.

## II. KEY CHALLENGES AND TRADE-OFFS

As mentioned earlier, the optimal 3D-positioning of even a single drone involves significant challenges with various trade-offs to be made. For example, a higher altitude of the drone implies a larger distance to the UEs, which in turn implies a larger path loss. On the other hand, when the drone is located at a higher altitude, there is a higher probability that the UEs have a Line-of-Sight link with the drone, which potentially reduces the path loss. But positioning the drone at a higher altitude also has another advantage, namely that UEs will be closer to the main lobe of the drone antenna. For illustrations of these effects we refer to Figures 2 and 3 which are based on the models explained in Section III.

Optimizing the altitude of the drone such that many UEs have a low path loss and high antenna gain, also comes with a downside as the drone may potentially be overloaded. In order to avoid this, we can offload some traffic to other cells by introducing a Cell Individual Offset (CIO) which makes the drone relatively less attractive to the UEs. On the other hand, this CIO can also be used to make the drone more attractive when only few UEs connect to it. Obviously, this introduces another control parameter whose optimal value depends on the position of the drone in a nontrivial manner.

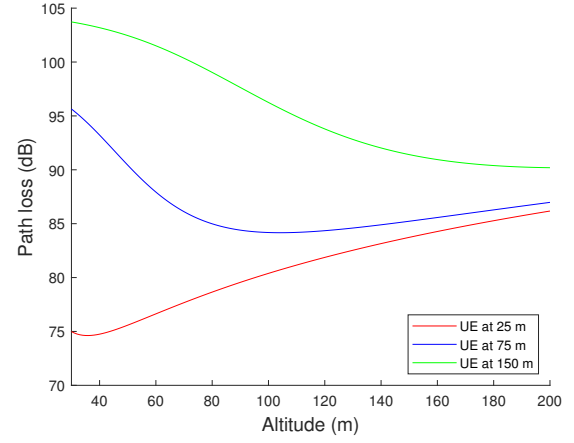


Fig. 2: Path loss at different altitudes of the drone for UEs at 25, 75 and 150 m horizontal distance.

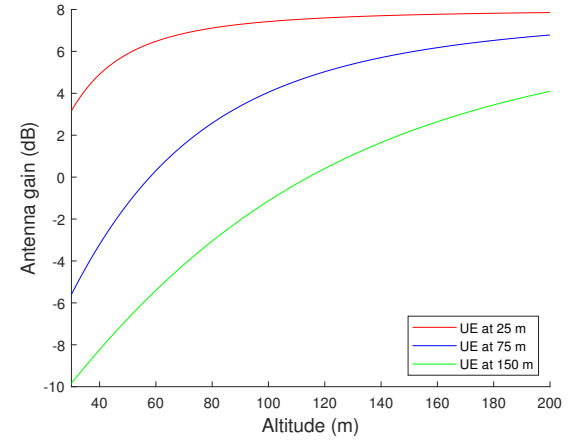


Fig. 3: Antenna gain at different altitudes of the drone for UEs at 25, 75 and 150 m horizontal distance.

Another challenge considered in this paper is to find the optimal position of the drone with respect to the location of a failing site and/or a traffic hotspot. For example, one could argue that it would be good to position the drone close to a failing base station to provide coverage to users that would require a large amount of radio resources otherwise. On the other hand, if there are areas with relatively many users, one could argue that it would be good to position a drone above such an area to ensure that these only require a small amount of radio resources.

## III. MODELING

In this section we will elaborate on the most important modeling aspects.

### A. Network and antenna aspects

We consider a hexagonal layout of twelve three-sectorised sites comprising  $12 \times 3 = 36$  cells served by directional antennas (see Figure 1a). A wraparound feature is applied to mimic an infinite-size network and avoid boundary effects. We

assume that the antennas are located at a height of 30 m [11] and that the inter-site distance is 500 m.

For the *regular base stations* we use the model proposed by [12] to represent horizontal and vertical components of the antenna gain of each sector as follows:

$$G_h(\varphi) = -\min \left\{ 12 \left( \frac{\varphi}{\text{HPBW}_h} \right)^2, \text{FBR}_h \right\} + G_m,$$

$$G_v(\theta) = \max \left\{ -12 \left( \frac{\theta - \theta_{\text{etilt}}}{\text{HPBW}_v} \right)^2, \text{SLL}_v \right\},$$

with the total antenna gain given by  $G(\varphi, \theta) = G_h(\varphi) + G_v(\theta)$ , where  $\text{HPBW}_{\{h,v\}}$  denotes the horizontal or vertical half-power beamwidth,  $G_m$  the maximum gain in dBi,  $\text{FBR}_h$  the front back ratio in dB, and  $\text{SLL}_v$  the side lobe level in dB, both relative to the maximum gain of the main beam. Furthermore  $\varphi$  denotes the horizontal angle relative to the azimuth direction,  $\theta$  the negative elevation angle relative to the horizontal plane, and  $\theta_{\text{etilt}}$  the electrical downtilt. In addition, we assume that these regular base stations each have a transmission power of  $P_m^{\text{Tot}} = 20$  W where the power of the reference signal  $P_m^{\text{RS}} = 1$  W.

For the *drone base station* we have rotated the model in [13, Table 7.3.1], and adapted the horizontal component to ensure a circular footprint, so that the antenna gain is modeled as

$$G(\theta) = -\min \left\{ 12 \left( \frac{\theta}{\text{HPBW}_d} \right)^2, \text{SLL}_d, \text{FBR}_d \right\} + G_d,$$

with similar notation as before. We assume that the drone base station has a transmission power of  $P_d^{\text{Tot}} = 0.5$  W where the power of the reference signal  $P_d^{\text{RS}} = 0.025$  W. Furthermore the drone is assumed to be connected to the backhaul network using another frequency range than the access.

### B. Propagation characteristics

To be able to model different kinds of urban scenarios, the ITU recommends three statistical parameters [14]:

- $\alpha$ : The ratio of built-up land area to the total land area.
- $\beta$ : The number of buildings per square kilometer.
- $\gamma$ : A scale parameter describing the buildings' heights according to a Rayleigh distribution.

As we consider a dense urban scenario we will set  $\alpha = 0.5$ ,  $\beta = 300$  and  $\gamma = 20$  [15].

For the *regular base stations*, we model the path loss according to the COST 231 Walfisch-Ikegami model [16]. We derive the parameters of this model using the statistical parameters  $\alpha$ ,  $\beta$  and  $\gamma$ . First the value of  $\gamma$  implies an average building height of  $\gamma\sqrt{\pi}/2$ . Following the reasoning in [15], the average width of the roads and the building separation are given by  $1000/\sqrt{\beta} - 1000\sqrt{\alpha/\beta}$  and  $1000/\sqrt{\beta}$ , respectively. Lastly, we take the road orientation with respect to the direct radio path to be 90 degrees as suggested in [16].

The COST 231 Walfisch-Ikegami model is only valid for transmitter heights up to 50 m. Therefore we model the path loss between a UE and the drone base station according to

the model described in [2], which is better suited for higher altitudes. This model considers two types of links, either having Line-of-Sight (LoS) or not (NLoS) with probabilities depending on the difference in height  $h$  and the horizontal distance  $r$  between the drone and UE. These probabilities are assumed to be

$$p_{\text{LoS}} = 1 - p_{\text{NLoS}} = \frac{1}{1 + \xi \exp(-\psi[\arctan(h/r) - \xi])},$$

where  $\xi = 12.081$  and  $\psi = 0.1139$  are environment parameters calculated according to the model in [2], which also uses the statistical parameters  $\alpha$ ,  $\beta$  and  $\gamma$ . Now the path loss is assumed to be the free-space path loss plus the excessive path loss  $\eta$  which depends on the type of link (LoS or NLoS). We take  $\eta_{\text{LoS}} = 1.6$  dB and  $\eta_{\text{NLoS}} = 23$  dB corresponding to a dense urban environment with a carrier frequency  $f = 2000$  MHz as reported in [15]. So the path loss is given by

$$L = -27.5522 + 20 \log_{10}(df) + p_{\text{LoS}}\eta_{\text{LoS}} + (1 - p_{\text{LoS}})\eta_{\text{NLoS}},$$

where the first two terms correspond to the free space path loss with  $d$  the 3D-distance between the drone and UE. We further impose a minimum coupling loss of 70 dB for all links [11].

### C. Traffic characteristics

We consider a single type of users initiating calls according to a spatial Poisson process. The occurrence of the disruptive event could result in an increased intensity of active users in an area close to the location of this event. We model such a hotspot as a circle with a radius of 100 meters, and assume that the intensity of initiated calls in the hotspot is a factor  $\rho$  times higher than elsewhere.

The calls have a mean duration of  $\tau$  seconds, and a minimum bit rate of  $R$  Mb/s throughout the duration of the call is required for it to be successfully completed.

### D. Resource management aspects

Upon arrival of a new call, it is first verified whether or not the user has coverage. For this we check whether there is at least one radio link with  $\text{RSRP} = P^{\text{RS}} + G - L > -120$  dBm, where  $G$  denotes the antenna gain and  $L$  the path loss. If this is the case, then this user is assigned to the access point with the highest value of  $\text{RSRP} + \text{CIO}$ , where the CIO is only included in the case of the drone base station.

An admission control mechanism accepts a new call when the estimated fraction of downlink resource blocks needed at the serving access point to satisfy all currently assigned users plus the new user remains below 98%. The 2% margin serves to cope with possible changes in the amount of interference.

To guarantee the minimum required bit rate of  $R$  Mb/s, we calculate the fraction of downlink resources that a user needs by  $R/(B \log_2(1 + \text{SINR}))$ , where  $B$  denotes the available bandwidth and SINR the Signal-to-Interference-plus-Noise Ratio of that user. For the calculation of the SINR, we assume a thermal noise of -106.94 dBm and a noise figure of 8 dB for each UE. Any surplus resources that are not needed to

TABLE I: Simulation parameters

General parameters		
$B$	Bandwidth	5 MHz
$h_{UE}$	Height of UE	1.5 m
$\lambda$	Arrival intensity (outside the hotspot)	2.1383 arrivals/s/km <sup>2</sup>
$\tau$	Average call duration	120 s
$R$	Minimum bit rate	0.05 Mb/s
Antenna gain - link with regular BS		
$G_m$	Maximum antenna gain	18 dBi
$HPBW_h$	Half-power beam width (horizontal)	65°
$HPBW_v$	Half-power beam width (vertical)	6.2°
$FBR_h$	Front back ratio	30 dB
$SLL_v$	Side lobe level	-18 dB
$\theta_{etilt}$	Electrical downtilt	8°
Antenna gain - link with drone BS		
$G_d$	Maximum antenna gain	8 dBi
$HPBW_d$	Half-power beam width	65°
$FBR_d$	Front-back ratio	30 dB
$SLL_d$	Side lobe level	30 dB

satisfy the minimum bit rate requirements are divided in a proportional fair way.

#### E. Performance measure

As mentioned earlier, we adopt the CSR as a key performance metric to capture the efficacy of the drone in ensuring coverage and offering capacity relief. We define the CSR as the fraction of calls that are successfully completed, meaning that the CSR is the fraction of users that has coverage and is admitted to the system. Note that the initial coverage and capacity checks imply that all admitted calls will be successfully completed. In evaluating the CSR, we only consider the users that in a normal situation would be served by the failing base station or in one of the six sectors adjacent to the sectors of the failing site.

### IV. SIMULATION RESULTS

We first list in Table I the simulation parameters that have not been introduced/specified earlier. These parameter values are based on the papers [12], [13], and our choice of a dense urban scenario. Furthermore, we have selected the parameters such that approximately 70% of the downlink resources are needed to guarantee the minimum bit rate for the admitted users in a scenario without a failing site and hotspot.

In all simulations, we measure the CSR over a period of 2000 seconds. As a warm-up period, we let each simulation run for a fixed, sufficiently long time to ensure measurements starting from a statistical equilibrium.

#### A. Impact of CIO and 3D position of the drone

We first investigate the performance impact of the altitude and CIO of the drone. We consider a scenario where the center of the hotspot is located 200 m from the failing site along one of its azimuth directions. Further suppose that the drone is positioned right above the center of the hotspot. In this experiment we vary the multiplication factor  $\rho$  for the traffic density in the hotspot, yielding the results shown in Figure 4.

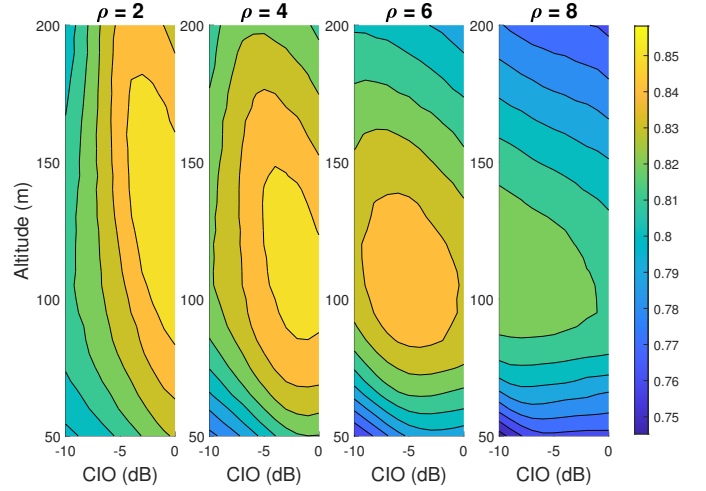


Fig. 4: CSR for different altitudes and CIO values of the drone.

Looking at Figure 4 we first note that as expected the CSR for the best combination of CIO and altitude decreases as  $\rho$  increases. We further see that both the optimal altitude and CIO of the drone decrease as  $\rho$  increases. This can be explained as the drone will try to serve as many users as possible, and to do so it needs to focus on the users that have the best SINR. For that we can choose to lower the CIO, which means that fewer users will be assigned to the drone, or reduce the altitude of the drone. The latter reduces the path loss of the users connected to the drone more than the antenna gain of these users, while at the same time ensuring that users with a relatively poor SINR will no longer be assigned to the drone (as their antenna gain reduces more than the path loss).

Another interesting observation is that the impact of the CIO on the CSR becomes smaller as  $\rho$  increases. On the other hand, the impact of the altitude on the CSR increases when  $\rho$  increases. However, the CSR is fairly insensitive to the control parameters near their optimal values, in particular for larger values of  $\rho$ .

As mentioned in Section II, it is not necessarily optimal to position the drone right above the hotspot. To investigate this, we fix the CIO to -4 dB and consider locations of the drone on a straight line from the failing site to the center of the hotspot, and plot in Figure 5 the CSR for different altitudes of the drone. We see that the optimal x,y-location is relatively close to the hotspot for  $\rho = 4$ , and near the location of the failing site for  $\rho = 2$ . This difference can be explained by the fact that moving towards the hotspot improves the channel quality of users in the hotspot, while at the same time the channel quality of users near the failing site degrades. Therefore, increasing the load of the hotspot implies that the benefits of relatively many of users in the hotspot will be greater, and thus the drone should move closer towards the center of the hotspot.

The key observation from Figures 4 and 5 is that there is not a universal optimal configuration of control parameters for all possible load scenarios. For example, the optimal configuration for  $\rho = 2$  has a higher CIO, higher altitude and a lower

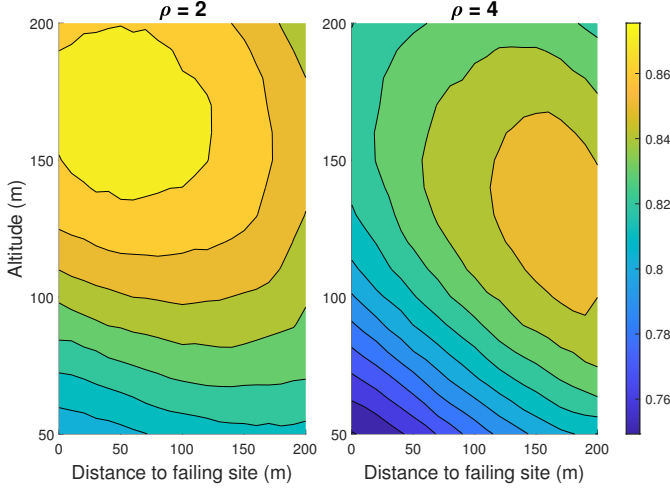


Fig. 5: CSR for different x,y-locations and altitudes of the drone.

horizontal distance to the failing site than for  $\rho = 4$ , and results in a distinctly suboptimal CSR when applied for  $\rho = 4$  or higher hotspot load densities.

### B. Optimal control parameters

In order to gain further insight in the optimal choices of x,y-coordinates, altitude and CIO, we conducted simulations for many possible configurations for each combination of  $\rho \in \{1, 2, 4, 6, 8\}$  and the distance of the hotspot to the failing site in  $\{0, 20, \dots, 200\}$ . For these experiments we first estimated a suitable range for the optimal control parameters using a few runs per combination. Then we estimated the CSR using 150 independent runs for each configuration of control parameters where we used a granularity of 5 meters for both the altitude and the distance between the drone and failing site and 0.5 dB for the CIO. In view of the insensitivity of the CSR near the optimal control parameter settings, we fitted the average simulated CSR for each value of  $\rho \in \{1, 2, 4, 6, 8\}$  using a quadratic function that takes as input the CIO, distance of the drone to the failing site, distance of the hotspot to the failing site and the altitude of the drone. For each fit we ensured that the optimal position of the drone is right above the failing site when the hotspot is centered at the failing site. Furthermore, we used over 1000 observations to determine 15 coefficients involved in this function. We compared the CSR provided by this function with the average values of the simulation results, and verified that the mean squared error is less than  $6 \cdot 10^{-7}$ , and in less than 2.5% of the used sets of control parameters the fit is outside a 95% confidence interval.

Figure 6 shows the maximum achievable CSR and Figures 7-9 show the corresponding configuration according to these fits, and indicates that the deployment of a drone does significantly improve the CSR. For example, we see improvements of at least 9, 10, 13, 16 and 19% for  $\rho = 1, 2, 4, 6$  and 8 respectively. This means that the fraction of failed calls would be approximately twice as high or higher without the

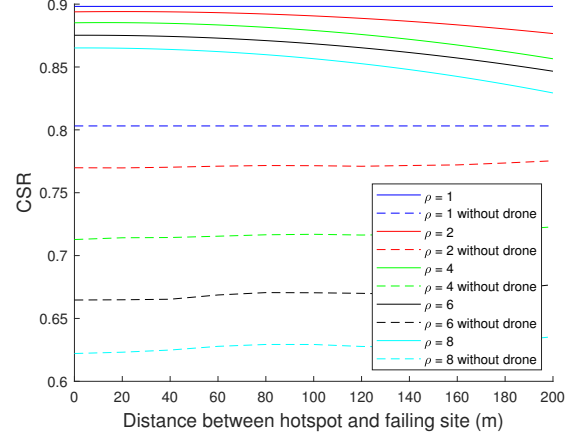


Fig. 6: Maximum achievable CSR as function of the horizontal distance between the hotspot and the failing site.

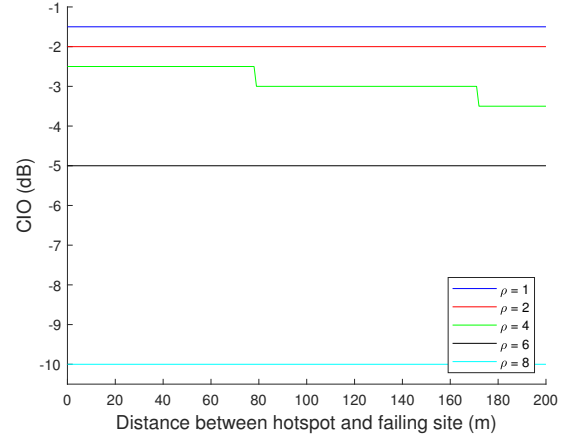


Fig. 7: Optimal CIO corresponding to the maximum achievable CSR as function of the horizontal distance between the hotspot and the failing site.

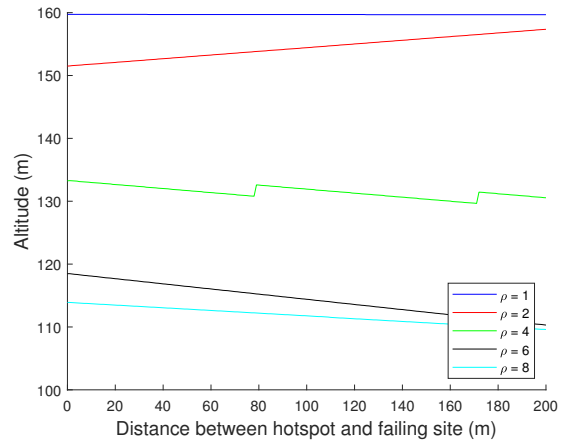


Fig. 8: Optimal altitude of the drone corresponding to the maximum achievable CSR as function of the horizontal distance between the hotspot and the failing site.



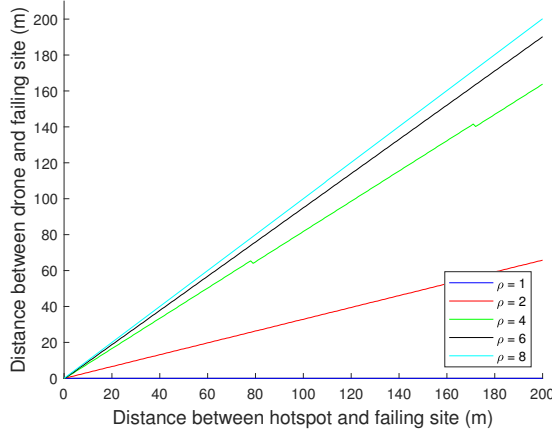


Fig. 9: Optimal horizontal distance between the drone and the failing site corresponding to the maximum achievable CSR as function of the horizontal distance between the hotspot and the failing site.

deployment of a drone. Additionally, the maximum achievable CSR decreases when the distance between the hotspot and the failing site increases, but also when traffic intensity in the hotspot increases.

We further observe that the optimal value of the CIO seems to depend only on the value of  $\rho$ , except for the jumps when  $\rho = 4$ . However, these jumps also suggest that there is a relation between the CIO and altitude, as the optimal altitude for  $\rho = 4$  jumps at the same points in the graph. Also the optimal distance between the drone and failing site shows a small jump at these points, however these jumps are relatively small. Finally, the optimal distance seems to increase linearly when the hotspot moves away from the failing site. In particular, the optimal position is close to the failing site and the hotspot for low and high load in the hotspot respectively.

A last observation is that the relative differences for the optimal distance between the drone and failing site differ more for small values of  $\rho$  while the relative differences for the optimal values of the CIO differ more for larger values of  $\rho$ . This can be explained by the fact that for higher values of  $\rho$  the optimal position of the drone is close to the center of the hotspot, meaning that the drone can not significantly improve the gains (antenna gain minus the path loss) of users in the hotspot by moving closer towards the hotspot. So the only way to serve more users is by steering users with relatively high resource requirements towards one of the regular base stations, which is done by lowering the CIO. On the other hand when  $\rho$  is small, we can improve the gains (antenna gain minus the path loss) of users in the hotspot by moving closer towards the hotspot. Therefore the drone is able to reduce the resource requirements of (relatively many) users in the hotspot by moving closer to the hotspot, which means that there is less need to steer users towards one of the regular base stations.

## V. CONCLUSION

We have investigated the impact of the position and selection bias of a drone base station on the performance of a cellular network in scenarios with a failing site and emerging hotspot. In these scenarios, we have seen that the deployment of a drone base station can significantly reduce the fraction of failed calls and observed that the CSR is not very sensitive to the control parameters when the selected configuration is close to the optimal setting. We further found that the optimal selection bias mostly depends on the traffic intensity in the hotspot, while the optimal position of the drone additionally depends on the location of the center of the hotspot.

It might be difficult in practice to accurately determine the location and/or traffic intensity in a hotspot. However, the relative insensitivity around the optimal settings of the control parameters is encouraging for the development of an adaptive algorithm with near-optimal performance, which is the topic of ongoing investigation.

## REFERENCES

- [1] 5G!Drones, EU H2020 project, [www.5gdrones.eu](http://www.5gdrones.eu), 2019-2022.
- [2] A. Al-Hourani, S. Kandeepan and S. Lardner, "Optimal LAP altitude for maximum coverage," in *IEEE Wireless Communications Letters*, vol. 3, no. 6, 2014.
- [3] R. Ghanavi, E. Kalantari, M. Sabbaghian, H. Yanikomeroglu and A. Yongacoglu, "Efficient 3D aerial base station placement considering users mobility by reinforcement learning," *2018 IEEE WCNC*, Barcelona, Spain, 2018.
- [4] P.V. Klaine, J.P.B. Nadas, R.D. Souza, and M.A. Imran "Distributed drone base station positioning for emergency cellular networks using reinforcement learning," *Cognitive Computing* vol. 10, 2018.
- [5] R. de Paula Parisotto, P.V. Klaine, J.P.B. Nadas, R.D. Souza, G. Brante and M.A. Imran, "Drone base station positioning and power allocation using reinforcement learning," *2019 ISWCS*, Oulu, Finland, 2019.
- [6] M. Mozaffari, W. Saad, M. Bennis and M. Debbah, "Drone small cells in the clouds: design, deployment and performance analysis," *2015 IEEE GLOBECOM*, San Diego, USA, 2015.
- [7] D. Prado, S. Inca, D. Martín-Sacristán and J. F. Monserrat, "Comparison of optimization methods for aerial base station placement with users mobility," *2019 EuCNC*, Valencia, Spain, 2019.
- [8] E. Kalantari, H. Yanikomeroglu and A. Yongacoglu, "On the number and 3D placement of drone base stations in wireless cellular networks," *2016 IEEE VTC-Fall*, Montreal, Canada, 2016.
- [9] N. Tafintsev, D. Moltchanov, S. Andreev, S. Yeh, N. Himayat, Y. Koucheryavy and M. Valkama, "Handling spontaneous traffic variations in 5G+ via offloading onto mmWave-capable UAV "bridges"," in *IEEE Transactions on Vehicular Technology*, vol. 69, no. 9, 2020.
- [10] M. Amirijoo, L. Jorguŝeski, R. Litjens and L.C. Schmelz, "Cell outage compensation in LTE networks: algorithms and performance assessment", *IWSON '11*, Budapest, Hungary, 2011.
- [11] 3GPP TR36.942: "Evolved universal terrestrial radio access (E-UTRA); radio frequency (RF) system scenarios". *3GPP Technical Report*, v16.0.0, 2020.
- [12] F. Gunnarsson, M.N. Johansson, A. Furuskär, M. Lundevall, A. Simonsson, C. Tildestav and M. Blomgren, "Downtilted base station antennas - a simulation model proposal and impact on HSPA and LTE performance." *2008 IEEE VTC-Fall*, Calgary, Canada, 2008.
- [13] 3GPP TR38.901: "Study on channel model for frequencies from 0.5 to 100 GHz". *3GPP Technical Report*, v16.1.0, 2019.
- [14] ITU-R, Rec. P1410-2 "Propagation data and prediction methods for the design of terrestrial broadband millimetric radio access systems." P Series, Radiowave Propagation, 2003.
- [15] A. Al-Hourani, S. Kandeepan and A. Jamalipour, "Modeling air-to-ground path loss for low altitude platforms in urban environments," *2014 IEEE GLOBECOM*, Austin, USA, 2014.
- [16] COST 231, Final report: "Digital mobile radio towards future generation systems.", 1999.